# Accepted Manuscript

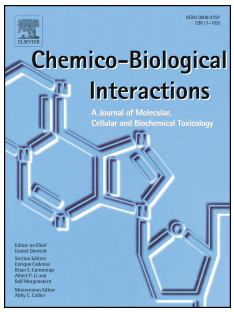


Structural aspects of 4-aminoquinolines as reversible inhibitors of human acetylcholinesterase and butyrylcholinesterase

Anita Bosak, Dejan M. Opsenica, Goran Šinko, Matija Zlatar, Zrinka Kovarik

PII: S0009-2797(19)30391-6

DOI: https://doi.org/10.1016/j.cbi.2019.05.024

Reference: CBI 8658

To appear in: *Chemico-Biological Interactions*

Received Date: 7 March 2019

Revised Date: 17 April 2019

Accepted Date: 13 May 2019

Please cite this article as: A. Bosak, D.M. Opsenica, G. Šinko, M. Zlatar, Z. Kovarik, Structural aspects of 4-aminoquinolines as reversible inhibitors of human acetylcholinesterase and butyrylcholinesterase, *Chemico-Biological Interactions* (2019), doi: https://doi.org/10.1016/j.cbi.2019.05.024.

# Structural aspects of 4-aminoquinolines as reversible inhibitors of human acetylcholinesterase and butyrylcholinesterase

Anita Bosak[a,*], Dejan M. Opsenica[b,*], Goran Šinko[a], Matija Zlatar[b], Zrinka Kovarik[a]

[a] *Institute for Medical Research and Occupational Health, Ksaverska cesta 2, 10000 Zagreb, Croatia*

[b] *Institute of Chemistry, Technology and Metallurgy, University of Belgrade, Studentski trg 12-16, 11000 Beograd, Serbia*

* Corresponding authors:

Dr Anita Bosak, Institute for Medical Research and Occupational Health, POBox 291, Ksaverska cesta 2, 10000 Zagreb, Croatia; e-mail: abosak@imi.hr

Dr Dejan M. Opsenica, Institute of Chemistry, Technology and Metallurgy, University of Belgrade, Studentski trg 12-16, 11000 Beograd, Serbia; e-mail: dopsen@chem.bg.ac.rs

**Abstract**:

Eight derivatives of 4-aminoquinolines differing in the substituents attached to the C(4)-amino group and C(7) were synthesised and tested as inhibitors of human acetylcholinesterase (AChE) and butyrylcholinesterase (BChE). Both enzymes were inhibited by all of the compounds with inhibition constants ($K_i$) ranging from 0.50 to 50 μM exhibiting slight selectivity toward AChE over BChE. The most potent inhibitors of AChE were compounds with an *n*-octylamino chain or adamantyl group. The shortening of the chain length resulted in a decrease in AChE inhibition by 5-20 times. Docking studies revealed that the quinoline group within the AChE active site was positioned in the choline binding site, while the C(4)-amino group substituents, depending on their lipophilicity, could establish hydrogen bonds or π-interactions with residues of the peripheral anionic site. The most potent inhibitors of BChE were compounds with the most voluminous substituent on C(4)-amino group (adamantyl) or those with a stronger electron withdrawing the substituent on C(7) (trifluormethyl group). Based on AChE inhibition, compounds with an *n*-octylamino chain or adamantyl substituent were shown to possess the capacity for further development as potential drugs for treatment of neurodegenerative diseases.

**Key words:** cholinesterase, Alzheimer's disease, p$K_a$ value, quinoline-based compounds, selectivity

## 1. Introduction

Derivatives of 4-aminoquinoline are one of the most used and most useful antimalarial agents in treating erythrocytic plasmodial infections from which chloroquine, hydroxychloroquine and amodiaquine are considered the most important drugs for the control and extermination of malaria. Apart from an original indication to prevent or cure malaria, these compounds also have anti-inflammatory, immunomodulating, anti-infective and antithrombotic activity, and have displayed metabolic effects and antitumoral properties [1]. Many studies have demonstrated that compounds based on a quinoline structure are potent inhibitors of both cholinesterases, acetylcholinesterase (AChE) and butyrylcholinesterase (BChE) [2, 3]. As their primary structural motive, these compounds have tacrine or quinidine moiety [4-9]. Furthermore, anticholinesterase activity has been confirmed for antimalarial drugs chloroquine, hydroxychloroquine and primaquine [10-12]. These compounds are derivatives of 4-aminoquinolines which were recently pointed out as a promising starting structural scaffold for the further design of novel multifunctional AChE inhibitors considering the simple structure and high inhibitory potency against AChE [13].

BChE and AChE are related enzymes that share more than 54% of their amino acid sequence and an active site located in a 20 Å deep gorge [14-16]. The active site of both AChE and BChE is divided into two sub-sites; the catalytic site (CAS) located close to the bottom of the gorge and the peripheral anionic site (PAS) located at the entrance of the gorge. CAS is composed of the catalytic triad, an oxyanion hole, an acyl-binding pocket and a choline binding site [17-19]. The active site of BChE differs in six out of the 14 aromatic residues lining AChE, which have aliphatic residues on corresponding places in BChE [16, 18, 19]. These differences lead to different interactions with the same substrates and ligands and defined AChE and BChE specificity and selectivity [20-24].

We synthesised eight derivatives of 4-aminoquinolines differing in the substituent attached to the C(4)-amino group and C(7) (Figure 1). The aim of this study was to test their inhibition potency toward human AChE and BChE, evaluate their inhibition selectivity and interpret obtained kinetic results by molecular modelling. Moreover, we evaluated the physicochemical properties of the tested compounds to estimate their capacity to penetrate the blood brain barrier.

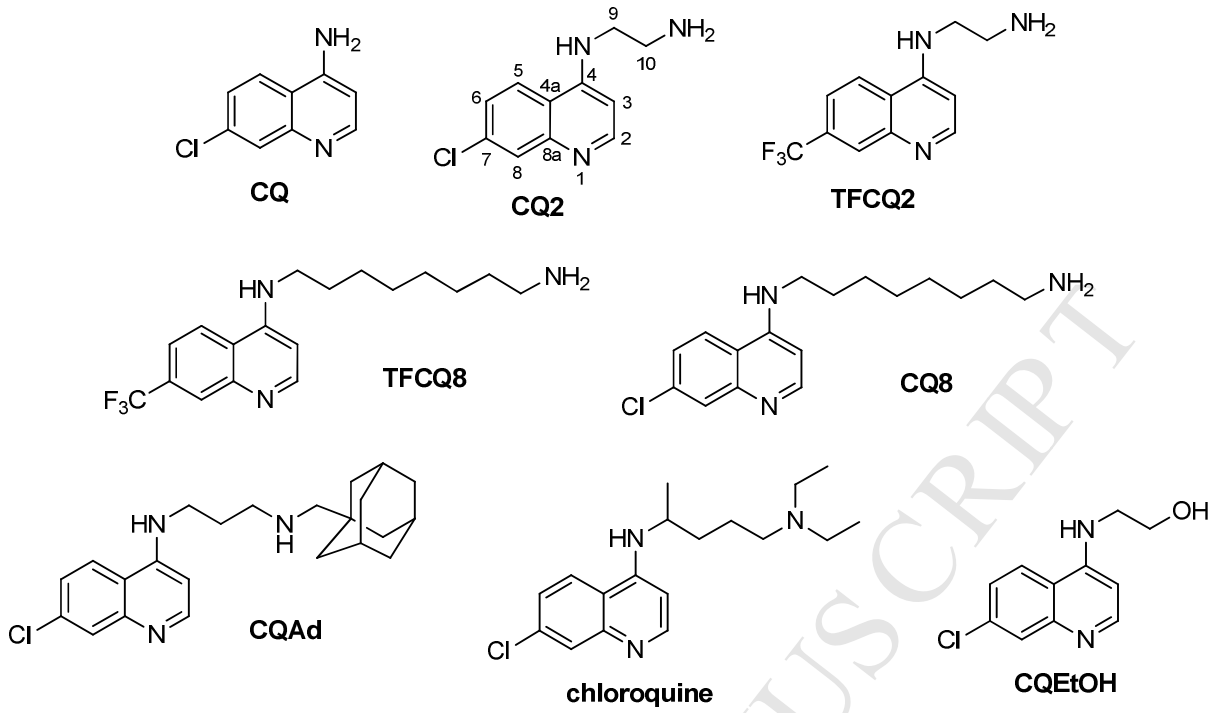


**Fig. 1.** Chemical structure of the tested compounds.

## 2. Materials and methods

### *2.1. Chemicals*

All of the chemicals, reagents and solvents for the preparation of 4-aminoquinoline derivatives were purchased from commercial sources. Acetylthiocholine (ATCh) and 5,5´-dithiobis(2-nitrobenzoic acid) (DTNB) were purchased from Sigma Chemical Co., USA. ATCh was dissolved in water and DTNB in 0.1 M sodium phosphate buffer (pH 7.4). 4-aminoquinilines were dissolved in DMSO and all further dilutions were made in water.

### *2.2. Enzymes*

Purified human BChE and recombinant human AChE were kindly provided by Dr Florian Nachon (Département de Toxicologie, Armed Forces Biomedical Research Institute, France). The concentration of the stock solution of enzymes (BChE: 5.6 µM; AChE: 0.20 µM) was determined as described previously [25]. The enzymes were diluted in a phosphate sodium buffer 0.1 M (pH 7.4) containing 0.1% BSA.

### *2.3. Synthesis*

The investigated compounds were synthetized as previously described [26, 27]. Briefly, the starting 4-chloroquinolines 1 or 2 were heated at 130 $^{o}$C in the presence of a corresponding amine (Scheme 1, route a), or $(NH_4)_2CO_3$ in phenole (Scheme1, route b), for defined reaction time. The reaction mixture was cooled at room temperature, water was added and crude product was filtered, rinsed with water, dried and prepare for purification by column chromatography (dry flash). For compound **CQ** reaction mixture in phenol was cooled to room temperature, ethyl-acetate was added and solution was washed with 0.1 M NaOH until excess of phenol was removed, twice with brine and dried over $Na_2SO_4$ anh. The solution was filtered, solvent was removed under reduced pressure and crude product was purified by column chromatography (dry flash). **CQAd** was obtained via reductive amination starting from adamantane-1-carbaldehyde and *N*-(7-chloroquinolin-4-yl)propane-1,3-diamine (compound 3, Scheme 1). After the complete consumption of the starting 3, the solvent was removed under reduced pressure and the final product was obtained after column chromatography (dry flash). **Chloroquine** was obtained after neutralisation of commercial drug chloroquine-diphosphate with 0.1 M NaOH. Obtained grounds were filtered of, rinsed with water and dried. The identity and purity of the obtained compounds were verified with corresponding spectral and analytical data (IR, NMR, HRMS, mp).

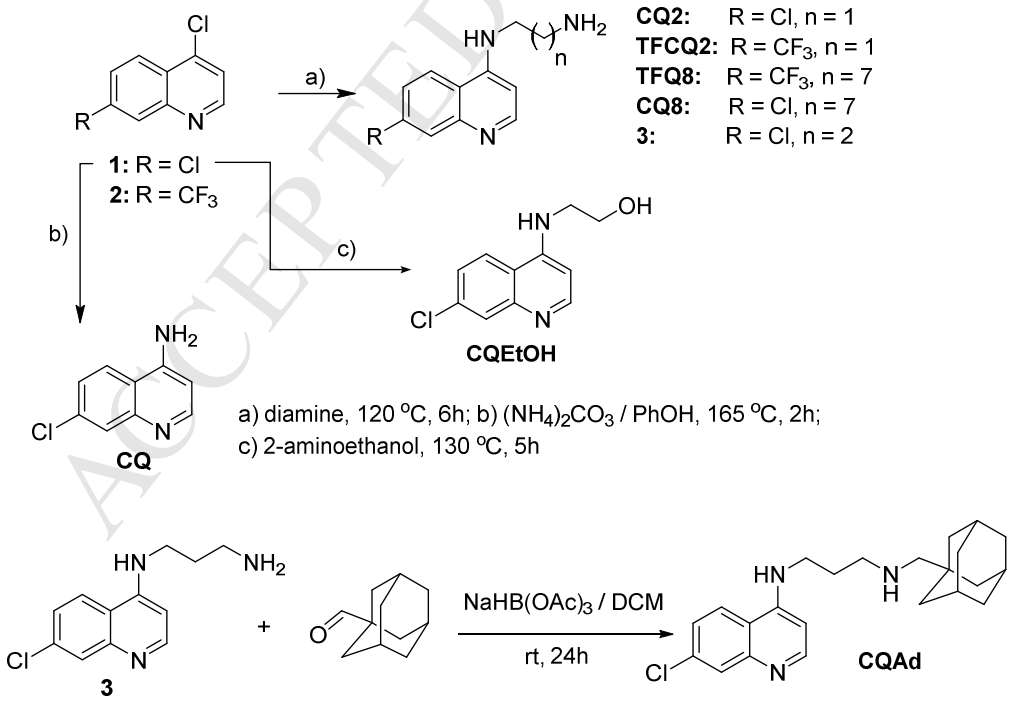


**Scheme 1.** Synthesis of 4-aminoquinoline derivatives.

*2.4. Inhibition measurements*

Enzyme activity was measured spectrophotometrically by the Ellman method using acetylthiocholine (ATCh; 0.050-0.50 mM) as substrate in 0.1 M phosphate buffer, pH 7.4 [28, 29]. The decrease of AChE and BChE activity towards ATCh was measured in the presence of aminoquinolines (final concentrations 0.25 - 200 μM, depending on the compound). The final content of DMSO in measurements was up to 0.2%. No side interactions of the tested compounds with ATCh or DTNB were detected. Measurements were done at 25 °C on a Tecan Infinite M200Pro plate reader (Austria).

The activities of the enzymes were measured at different substrate concentrations ($s$) in the absence ($v_0$) and presence ($v_i$) of a given aminoquinolines concentration ($i$) selected to inhibit the enzymes for 20 - 80%. At least three concentrations of inhibitors for each substrate concentration were used in at least two experiments. The apparent inhibition constant ($K_{i,app}$) was calculated using the Hunter-Downs equation and the linear regression analysis [30]:

$$K_{i,app} = v_i \cdot i / (v_0 - v_i) = K_i + K_i / K_{(s)} \cdot s \quad (1)$$

where y-intercept determines the enzyme-inhibitor dissociation constants ($K_i$), while x-intercept determines the enzyme-substrate dissociation constant, $K_{(S)}$. The equation was used with the assumption that the substrate, due to low substrate concentrations used in experiments, binds only to the catalytic site, while the inhibitor can bind to both sites, catalytic and peripheral site [30].

The determination of kinetic constants was carried out using the GraphPad Prism 6.0 software (GraphPad Software, San Diego, USA).

*2.5. p$K_a$ determination*

The p$K_a$ values were obtained adhering to density functional theory (DFT) based linear regression approach [31-35]. The p$K_a$ values are computed by:

$$pK_a = m\Delta G + C \quad (2)$$

where ΔG is a difference in Gibbs free energy between a deprotonated amine and its conjugated acid in aqueous solution at 298.15 K. The linear regression parameters $m$ and $C$ are found by a linear fit of $pK_a^{exp}$ values for a training set of compounds and their calculated ΔG. The ΔG were calculated at LC-wPBE/6-31G+(d) level of theory with the continuum solvation model based on density (SMD) [36] using the default settings in Gaussian09 [37]

and water as a solvent. Thermal corrections to the free energy were computed using the ideal gas molecular partition functions in conjunction with the quasi-harmonic entropy correction as proposed by Grimme [38] with the GoodVibes program v2.0.1 [39]. A conformational search was done for each molecule, and the conformers with the lowest free energy were selected for p$K_a$ estimation. Initial conformations were generated using Open Babel's Confab algorithm [40]. For symmetric diamines the statistical correction of 2.303RTln(2), where R is the gas constant and T is the temperature, was added to the calculated ΔG for the estimation of the first p$K_a$ and subtracted from the calculated ΔG for the estimation of the second p$K_a$ [41, 42]. At 298.15 K this correction equals 1.1795 kJ/mol. Finally, the calculated ΔG values of investigated 4-aminoquinolines were used for the estimation of their p$K_a$ values applying the equation 2. Details of applied methods, structure of amines used for preparing of test and control set of compounds and graphics are given in the Supplementary Material.

### *2.6. Molecular modelling*

The crystal structure of human BChE and human AChE deposited in Protein Data Bank, PDB code 2PM8 [43] and 4PQE [44], respectively, were used. The CDOCKER protocol based on the CHARMm force field (Accelrys Discovery Studio 2017R2 software, San Diego, USA) was used for docking as described previously [45].

### *2.7. In silico prediction of blood-brain barrier (BBB) penetration*

The BBB permeability potential was evaluated by molecular descriptors: the calculated logarithm of the octanol/water partition coefficient (logP), the molecular weight (MW), the polar surface area (PSA), the number of hydrogen bond donors (HBD), the number of hydrogen bond acceptors (HBA) and the number of rotable bonds (RB), which were determined *in silico* using the Chemicalize 2018 platform [46]. The obtained results were compared to the recommendations of physicochemical properties for successful central nervous system drugs [47].

## 3. Results and discussion

Eight derivatives of quinoline were synthesized following procedures described previously [27, 28] with moderate to good yields. Compounds differ in the substituent attached to the C(4)-amino group and C(7) of 4-aminoquinoline (Fig. 1).

The p$K_a$ values of 4-aminoquinolines were evaluated *in silico* to estimate their acid/base character (Table 1). The reliability of the applied method for p$K_a$ calculation was confirmed with low Mean absolute error (MAE) 0.20 p$K_a$ units and Maximum absolute error (Max AE) 0.51 p$K_a$ units, and both were far lower than the values currently targeted in the calculation of p$K_a$ [31, 32]. According to determined p$K_a$ values, at physiological pH, the terminal amino-group on C(4)-*N*-substituent in all tested compounds (p$K_{a2\ calc.}$) was protonated. The p$K_a$ value of the aromatic nitrogen from quinoline ring (p$K_{a1\ calc.}$) was within 7.05 - 8.37 and both the protonated and the non-protonated form co-existed simultaneously. However, at physiological pH, the majority of the tested compounds existed dominantly, within 76-90%, in a form where the nitrogen in the quinoline ring was protonated (double protonated form), while for compounds **CQ2** and **TFCQ2** the nitrogen was dominantly deprotonated (62 and 69%, respectively; mono protonated form).

**Table 1.** Calculated p$K_a$ values for the tested compounds.

| Compound | p$K_{a1\ calc.}$ (quinoline) | p$K_{a2\ calc.}$ (terminal amino-group) |
|---|---|---|
| **CQ** | 8.33[a] | - |
| **CQ2** | 7.19 | 9.11 |
| **TFQ2** | 7.05 | 8.81 |
| **CQ8** | 8.37 | 10.31 |
| **TFQ8** | 7.90 | 10.41 |
| **CQAd** | 7.96 | 10.53 |
| **chloroquine** | 8.08[b] | 10.77[b] |
| **CQEtOH** | 8.16 | - |

[a] ref. [48]
[b] ref. [49**]**

All of the tested 4-aminoquinolines reversibly inhibited the activity of both, AChE and BChE, forming noncovalent interactions within the active site of the enzymes. As a measure of their inhibition potency, we determined the dissociation constants (± standard errors) of the enzyme-inhibitor complex ($K_i$; Table 2).

The AChE activity was inhibited with $K_i$ constants ranging from 0.46-11 μM (Table 2). AChE displayed the highest affinity toward compounds with *n*-octylamino (**TFQ8** and **CQ8**) and adamantyl group (**CQAd**) substituted the C(4)-amino group, demonstrating that high lipophilic substituent, represented with long alkyl chain or adamantyl-group on C(4)-amino group, is important for achieving high inhibition potency. Our observation is supported by the fact that AChE displayed the lowest affinity toward **CQ** having no substituent on the C(4)-amino group, and which has a 2.7, 14 and 18 times lower inhibition potency in comparison to **CQ2**, **CQAd** and **CQ8**, respectively. Introduction of a hydroxyethyl group on C(4)-amino group, as it is in **CQEtOH**, gave an indication about the importance of the presence of a basic amino group for achieving a higher inhibition potency. The replacement of a terminal amino group in **CQ2** with hydroxyl, as it is in **CQEtOH**, caused about a twofold decrease of inhibition potency compared to **CQ2**. Interestingly, the 2.5-fold increase in inhibition of AChE, in comparison to **CQ**, was achieved with **chloroquine** although the size and the lipophilicity of substituent in **chloroquine** were comparable with that of **TFQ8**, **CQ8** and **CQAd**. It seems that the branching of the substituent on the C(4)-amino group (the methyl group on C(10) and the *N*,*N*-diethyl terminal group) in **chloroquine** decreased the

inhibition potency toward AChE. The replacement of chlorine with stronger electron-withdrawing trifluoromethyl group on C(7) did not affect the inhibition potency of the tested 4-aminoquinolines indicating a minor role of C(7) substituent on AChE inhibition. That is illustrated with almost identical $K_i$ values for corresponding pairs of substituents, i.e. **CQ2** *vs.* **TFQ2**, and **C8** *vs.* **TFQ8**. The connection of the size of the C(4)-amino group and the inhibition potency toward AChE was previously shown for antimalarials chloroquine, amopyroquine and amodiaquine. Amodiaquine and amopyroquine, with a phenyl substituent on the C(4)-amino group, were more potent inhibitors of electric eel AChE than chloroquine with an aliphatic substituent [10]. The $K_i$ for **chloroquine** (Table 2) corresponds to a previously reported value for human erythrocyte AChE as well to that for electric eel AChE [10, 11].

We evaluated the type of inhibition, whether is competitive, non-competitive or mixed, from the slope at the inhibition plots and dissociation constants of the enzyme-substrate complex ($K_s$; Table 2). For majority of tested compounds, the slope was higher than zero (i.e. $K_{i,app}$ proportionally depended on substrate concentration) and the $K_s$ values corresponded to previously determined Michaelis-Menten constant ($K_M$) [30] implying a competitive inhibition and binding of the tested compounds to the catalytic site of AChE. For two compounds with a trifluoromethyl group (**TFQ2** and **TFQ8**), and **CQ8** the slope was close to zero indicating no binding competition with the substrate in the catalytic site, and a non-competitive type of inhibition (i.e. binding of those compounds in PAS). In the case of **CQAd** we observed a deviation from linearity suggesting a mixed type of inhibition due to its binding to both catalytic site and PAS of AChE.

To evaluate binding interactions we performed docking simulations with mono and double protonated form of amine group from a quinoline ring because no correlation between p$K_a$ values (Table 1) and inhibition potency (Table 2) was observed. Indeed, docking results confirmed these results and showed that the double protonated and mono protonated form of the compounds had a very similar orientation of ligands within the active site with CDOCKER energies for double protonated forms about 10 kcal/mol lower than the corresponding mono protonated forms

**Table 2.** Reversible inhibition of recombinant human AChE and human BChE by 4-aminoquinolines. The enzyme-inhibitor complex dissociation constant ($K_i \pm$ SE) was determined by linear regression from $K_{i,app}$ constants obtained from at least three experiments at 25°C. *c*, *n* and *m* stands for competitive, non-competitive and mixed type of inhibition, respectively

| **Compound** | **AChE** | | | **BChE** | | | $K_i$(BChE)/$K_i$(AChE) |
|---|---|---|---|---|---|---|---|
| | [I], (μM) | $K_i$, (μM) | $K_s$, (mM) | [I], (μM) | $K_i$, (μM) | $K_s$, (mM) | |
| **CQ** | 2-40 | 11±0.3 (c) | 0.48±0.03 | 20-60 | 31±7 (c) | 0.15±0.04 | 2.8 |
| **CQ2** | 2-10 | 4.1±0.2 (c) | 0.78±0.14 | 10-40 | 12± 1 (c) | 0.53±0.08 | 2.9 |
| **CQ8** | 0.25-10 | 0.61±0.03 (n) | - | 2-20 | 6.1±0.9 (c) | 0.26±0.04 | 10 |
| **TFQ2** | 2-10 | 3.6±0.2 (n) | - | 2-10 | 2.5±0.3 (c) | 0.61±0.15 | 0.69 |
| **TFQ8** | 0.25-2 | 0.46±0.01 (n) | - | 1-20 | 1.9±0.3 (c) | 0.24±0.05 | 4.1 |
| **CQAd** | 0.50-1.5 | 0.77±0.09 (m) | 0.45±0.10 | 2-8 | 3.2±0.4 (m) | 3.1±0.4 | 4.2 |
| **CQEtOH** | 5-50 | 10±1 (c) | 0.95±0.19 | 40-200 | 51±8 (c) | 0.21±0.04 | 5.1 |
| **chloroquine** | 2-10 | 4.0±0.2 (c) | 1.0±0.2 | 5-20 | 7.2±1.7 (c) | 0.27±0.05 | 1.8 |

Key interactions between residues in the active site of both cholinesterases and the tested 4-aminoquinilines are listed in Table 3. Molecular docking showed that Trp86 in AChE, and the corresponding Trp82 in BChE, were the key residues for stabilisation of 4-aminoquinoline moiety in the choline binding site, as shown previously for tacrine and huprine, potent cholinesterase inhibitors [4, 50, 51]. The orientation of the quinoline group within the AChE active site was governed, along with Trp86, by forming interactions with Tyr337 and/or Tyr341 from the choline binding site. Also, all of the tested ligands (except **CQ)** were stabilized via H-bonding and/or π-interactions with Tyr72, Tyr124 or Trp286 from the peripheral anionic site (Table 3, Fig. 2). It is worthy of noting that molecular docking confirmed the evaluation of dissociation constants (cf. Table 2), and interactions of non-competitive (**TFQ2**, **TFQ**, and **CQ8**), and mixed type (**CQAd**) inhibitors with residues from PAS. However, the determined inhibition potency of the tested 4-aminoquinolines can be attributed to additional stabilisation of substituents on the C(4)-amino group with residues in the AChE active site. For example, substituents on the C(4)-amino group of **CQAd** and **chloroquine** formed a salt bridge with Asp74, a residue in PAS involved in substrate trafficking down the gorge during hydrolytic processes (Fig. 2) [52].

**Table 3.** Key interactions in the human AChE (HuAChE, accession no. P22303) and human BChE (HuBChE, accession no. P06267) active site gorge evaluated by molecular docking.

| **Compound** | **AChE** | | | **BChE** | | |
|---|---|---|---|---|---|---|
| | **H-bond** | **π-orbitals** | **other** | **H-bond** | **π-orbitals** | **other** |
| TFQ2 | Tyr337, Ser125,Gln71, His447,Gly448, Asn87 Tyr72 | Trp86, His447 | Glu202 (Halogen acceptor) | Trp82, Glu197, Tyr128, Gly115, Ser198 | His438 | Gly116, Gly117 (Amide-π stacked), Pro285, Leu286 (Halogen acceptor) |
| TFQ8 | Arg291, His447, Gly448, Ser125, Tyr341, Asp74, Tyr124 | Trp86, His447 | Glu202 (Halogen acceptor) | Tyr128, Ser198, Thr120, His438, Gly439, Trp82 | Trp82 | Glu197, Ser198 (Halogen acceptor) |
| CQ | Tyr337, His447 | Trp86, Tyr337, His447 | | Gly115, Glu197 His438 | Trp82 | |
| CQEtOH | Asp74, Ser125, Tyr124, His447, Tyr341, Asn87, Tyr337 | Trp86, His447 | | Ser198, Glu197 His438 | Phe329, Trp231 | Leu286 (Hydrophobic) |
| CQ2 | Ser125, Gln71, Tyr341, Asn87, Tyr72, Tyr337 | Trp86, His447 | | Ser198, Thr120 Trp231 | Trp82, His438 | Gly116, Gly117 (Amide-π stacked) |
| CQ8 | Asp74, Glu202, Phe295, Tyr337, Tyr341 | Tyr124, Trp286, Tyr341 | Glu202 (Salt bridge) | Glu197, His438 | Trp82, His438, Phe329, Trp430 | Ala328 |
| chloroquine | Tyr124, Trp86, Ser125 | Trp86, Tyr341 | Asp74 (Salt bridge) | His438 | Trp82, Tyr332 | Glu197 (Salt bridge), Pro285, Phe329, Tyr332 (Hydrophobic) |
| CQAd | Tyr124, Thr83, Tyr337 | Trp86, Trp286, Tyr337, Tyr72, His447 | Asp74, (Salt bridge) | Glu197, His438, Ser198 | Trp82, Tyr332 | Glu197 (Salt bridge), Gly116, Gly117 (Amide-π stacked), Ala328 (Hydrophobic) |

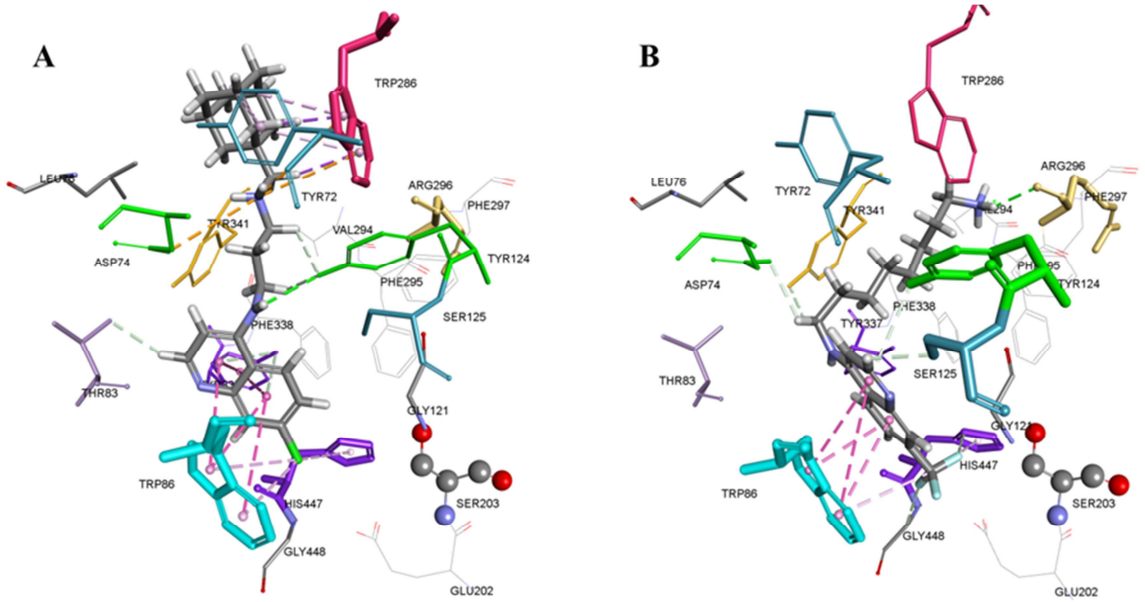


**Fig. 2.** Orientation of ligands in the active site of AChE. Position of ligand **CQAd** (A) and ligand **TFQ8** (B). Interactions are presented in green (H-bonds), orange (cation-π interaction), and purple (hydrophobic interactions).

The most potent inhibitors of BChE were compounds with the most voluminous substituent on the C(4)-amino group (**CQAd**) or with an electron-withdrawing group on C(7) (**TFQ2** and **TFQ8**). In other words, the substitution of the trifluoromethyl group in **TFQ8** and **TFQ2** by chlorine, as in **CQ8** and **CQ2**, respectively, caused a 5 or 2-fold, decrease of their inhibition potency. On the other hand, substitution of adamantly group in **CQAd** with diethylamino group, as in **chloroquine**, caused a 2-fold decrease in the inhibition potency. Further reduction of the size of substituent on C(4)-amine group in compounds **CQ** and **CQEtOH** led to an additional 10 times decrease of BChE affinity. Additionally, the $K_s$ values for all compounds (Table 2) corresponded to BChE's previously determined Michaelis-Menten constant ($K_M$) [30], suggesting a competitive binding of the tested compounds to the catalytic site of BChE. A mixed type inhibition was determined only for **CQAd**. Again, similarly to AChE, no correlation between the acid/base character of 4-aminoquinolines and their inhibition potency towards BChE was observed.

Molecular modelling of the tested compounds in BChE revealed a general involvement of Trp82 from the choline binding site in ligand stabilisation together with Trp231 from the acyl pocket, amide group of Gly116 and Gly117 from the oxyanion hole, His438 from the catalytic triad, and Thr120 via π-stacking and H-bonding (Table 3). Interactions with Pro285 and Leu286 as halogen acceptors were observed for **TFQ2**, **CQEtOH**, and **chloroquine**. The

interaction with Trp231 seems important for the 4-fold increased affinity of **CQ2** compared to **CQEtOH,** compounds that have the amino group versus hydroxyl group on the C(4)-amino substituent, respectively (Fig. 3). Similarly, Košak et al. demonstrated that the same replacement of a hydroxyl group by an amino group in ligands increased BChE affinity up to picomolar range due to the interaction of an amino group with Trp231 [53]. Moreover, interactions with Trp231 and Trp82 have been proven to be decisive for ethopropazine selectivity toward BChE [54], and for potent dual binding inhibitors [55]. It seems that Trp231 has a similar role in ligand stabilisation as Trp286 from PAS in AChE [53].

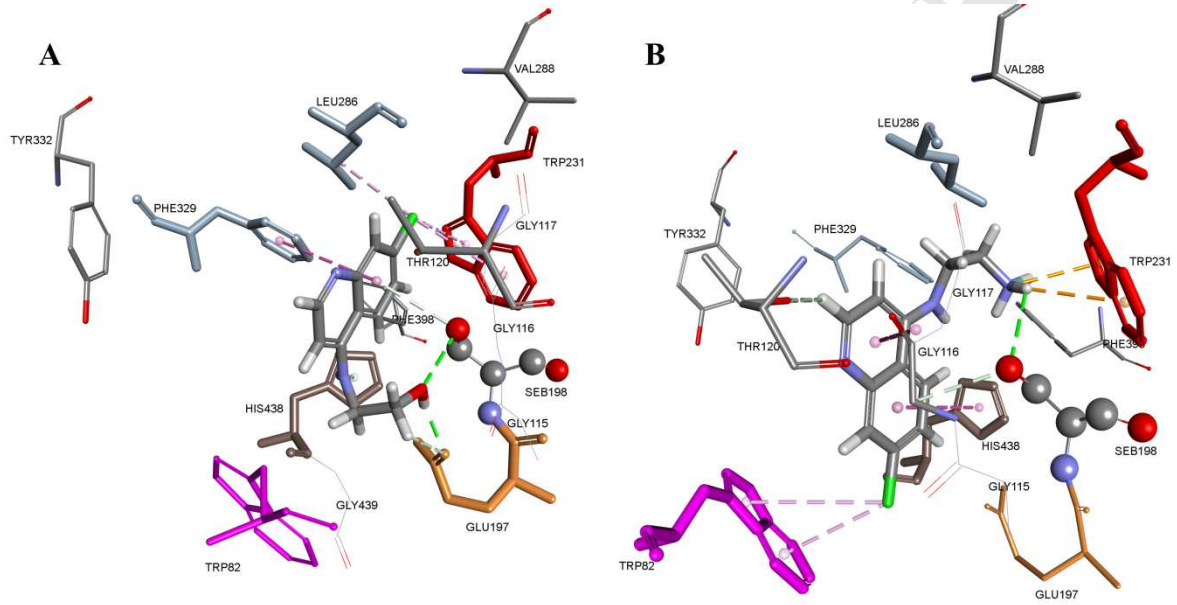


**Fig. 3.** Position of ligand **CQEtOH** (A) and ligand **CQ2** (B) in the active site of BChE. Interactions are presented in green (H-bonds), orange (cation-π interaction) and purple (hydrophobic interactions).

The inhibition selectivity of the compounds was defined with the ratio of $K_i$ constants of AChE and BChE (Table 2). Overall, all of the compounds had a 1.8 to 10 times higher preference for AChE over BChE, except **TFQ2**, the compound with a trifluoromethyl group on C(7) and an ethylamino substituent on the C(4)-amino group, which exhibited a 1.4 times higher preference for BChE. The highest selectivity was displayed by **CQ8**, a compound with an *n*-octylamino substituent on the C(4)-amino group and chlorine on the C(7). The determined selectivity was comparable to that of galantamine which had about a 9 times higher preference for human AChE over BChE [56].

Molecular modelling of the most selective inhibitor, **CQ8**, showed that the largest difference in its accommodation in the active site of AChE and BChE was the positioning of quinoline moiety (Fig 4). In AChE, it was stabilised with residues Tyr124, Trp286, and Tyr341, while in BChE with aromatic residues of Trp82, Phe329 and Trp430. Moreover, **CQ8** in AChE was in extended form, and the protonated amino group was stabilised with Trp86 and Glu202 (Fig 4A). Larger BChE active site allows bent conformation of **CQ8** and the protonated amino group is stabilised with Glu197 and His438 (Fig. 4B).

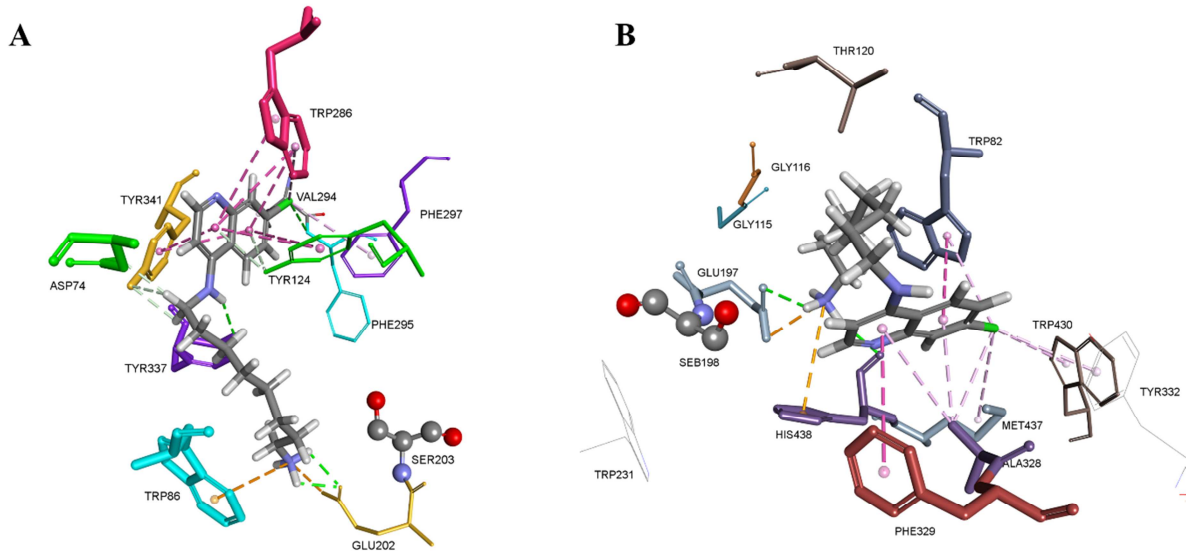


**Fig. 4.** Comparison of ligand **CQ8** orientations in the active site of cholinesterases. Position of ligand in AChE (A) and in BChE (B). Interactions are presented in green (H-bonds), orange (cation-π interaction) and purple (hydrophobic interactions).

Since blood brain barrier (BBB) penetration is a key request for the selection of compounds for further refinement of potentially centrally active drugs, we estimated the *in silico* ability of the tested compounds to cross the BBB. Figure 5 shows the radar plot of six physicochemical properties of the tested 4-aminoquinolines in relation to recommended values of CNS-active drugs, which generally have lower molecular weight (MW<450), have moderate hydrophobicity (logP<5), have fewer hydrogen bonds donors and acceptors (HBD< 3 and HBA<7), fewer rotatable bonds (RB<8) and are less polar (polar surface area PSA<70 $Å^2$) than drugs that are not active in CNS [47]. All of the tested 4-aminoquinolines had optimal values of lipophilicity (logP = 1.4 − 4.3), molecular weight (180 − 384 g/mol), polar

surface area (up to 50.94 Å2), and optimal numbers of H-bond donors (max 2) and H-bond acceptors (max 3). Molecular flexibility, as characterized by the number of rotatable bonds (0 − 10), was favourable in five out of eight compounds. Moreover, the p$K_a$ value of the most basic group (amine on C(4)-amino substituent) was also considered as a molecular descriptor whose value for CNS drugs is limited to 7.5 – 10.5 [47]. Accordingly the p$K_{a\ calc.}$ values cf. (Table 1) are within or close to recommended range (8.08 − 10.5). Nevertheless, the above results suggest that all of the tested 4-aminoquinilines have potential to penetrate the BBB and present a solid starting point for further structural refinement in terms of developing CNS-active drugs.

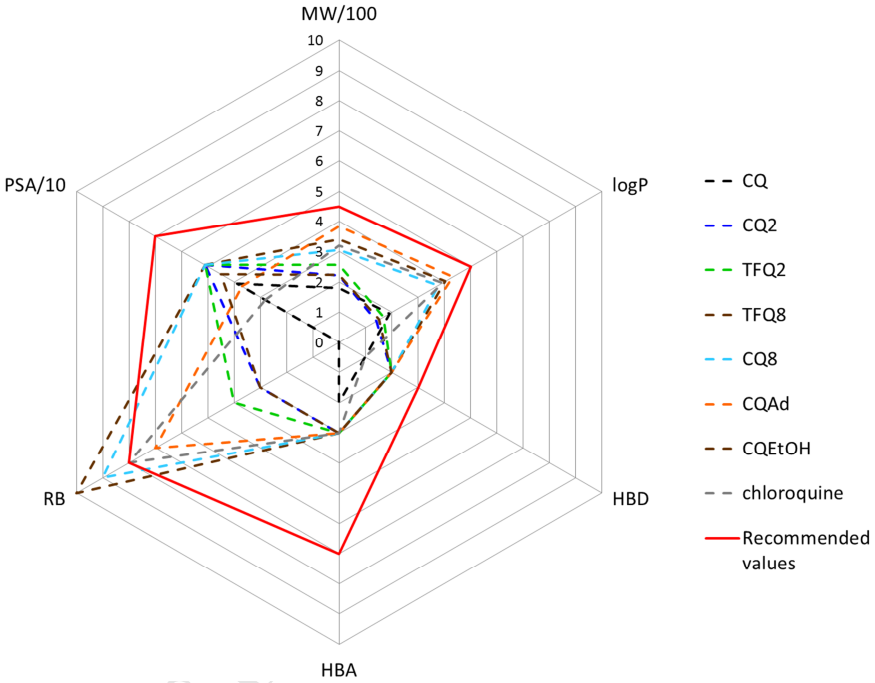


**Fig. 5.** Radar plot of physicochemical properties (molecular weight, MW; lipophilicity coefficient, logP; number of hydrogen bonds donors, HBD, and acceptors HBA; rotatable bonds, RB; polar surface area, PSA) of the tested 4-aminoquinolines. Recommended values for the CNS-active drugs are presented by a red line [47].

## 4. Conclusions

Out of eight tested derivatives of 4-aminoquinoline that differ in C(4) and/or C(7) substituents, the most potent inhibitors of AChE, in lower micromolar range, were compounds with an *n*-aminooctyl chain (**CQ8**) or adamantyl group (**CQAd**), regardless of the substituent in position C(7). For BChE, the most potent inhibitors were **CQ8** and derivatives with trifluoromethyl group on C(7) (**TFQ2** and **TFQ8**). Molecular modelling showed that one of

the most potent inhibitors of both AChE and BChE, as well as the most selective AChE inhibitor, **CQ8**, was positioned in AChE in extended form, while in BChE it was in a bent conformation. The studied derivatives of 4-aminoquinolies provided a solid starting core for further design of novel cholinesterase inhibitors, either as peripherally active drugs for treatment of Myasthenia gravis, or as centrally active drugs for use in treatment of neurodegenerative diseases like AD. Also, an additional advantage of such compounds is their simple structure and low logP which allows further structural refinement in terms of drugability.

**Conflict of interest statement**

The authors declare that there are no conflicts of interest.

**Acknowledgment**: The authors are grateful to Dr Florian Nachon for the human recombinant AChE and human purified BChE, and Makso Herman for language editing. This study was financed by the Croatian Science Foundation (IP-2018-01-7683) and Ministry of Education, Science and Technological Development of Serbia (Grants no. 172008 and 172035), and by the Institute for Medical Research and Occupational Health project to A.B.

**References**

[1] D. Plantone, T. Koudriavtseva, Current and future use of chloroquine and hydroxychloroquine in infectious, immune, neoplastic, and neurological diseases: A mini-review, Clin. Drug Investig. 38(8) (2018) 653-671. https://doi.org/10.1007/s40261-018-0656-y

[2] S.-S. Xie, X.-B. Wang, J.-Y. Li, L. Yang, L.-Y. Kong, Design, synthesis and evaluation of novel tacrine-coumarin hybrids as multifunctional cholinesterase inhibitors against Alzheimer's disease, Eur. J. Med. Chem. 64 (2013) 540-553. https://dx.doi.org/10.1016/j.ejmech.2013.03.051.

[3] S. Hamulakova, L. Janovec, O. Soukup, D. Jun, J. Janockova, M. Hrabinova, V. Sepsova, K. Kuca, Tacrine-coumarin and tacrine-7-chloroquinoline hybrids with thiourea linkers: cholinesterase inhibition properties, kinetic study, molecular docking and permeability assay for blood-brain barrier, Curr. Alzheimer Res. 15(12) (2018)1096-1105. https://doi.org/10.2174/1567205015666180711110750.

[4] M. Harel, I. Schalk, L. Ehret-Sabatier, F. Bouet, M. Goeldner, C. Hirth, P.H. Axelsen, I. Silman, J.L. Sussman, Quaternary ligand binding to aromatic residues in the active-site gorge of acetylcholinesterase, Proc. Natl. Acad. Sci. USA. 90(19) (1993) 9031-9035.

[5] E.H. Rydberg, B. Brumshtein, H.M. Greenblatt, D.M. Wong, D. Shaya, L.D. Williams, P.R. Carlier, Y.P. Pang, I. Silman, J.L. Sussman, Complexes of alkylene-linked tacrine dimers with Torpedo californica acetylcholinesterase: Binding of Bis5-tacrine produces a dramatic rearrangement in the active-site gorge, J. Med. Chem. 49(18) (2006) 5491-500. https://doi.org/10.1021/jm060164b.

[6] M. Harel, G. Kryger, T.L. Rosenberry, W.D. Mallender, T. Lewis, R.J. Fletcher, J.M. Guss, I. Silman, J.L. Sussman, Three-dimensional structures of Drosophila melanogaster acetylcholinesterase and of its complexes with two potent inhibitors, Protein Sci. 9(6) (2000) https://doi.org/1063-1072.10.1110/ps.9.6.1063.

[7] A. Bosak, A. Ramic, T. Smidlehner, T. Hrenar, I. Primozic, Z. Kovarik, 2018. Design and evaluation of selective butyrylcholinesterase inhibitors based on Cinchona alkaloid scaffold, Plos One 13(10), e0205193. https://doi.org/10.1371/journal.pone.0205193..

[8] D. Karlsson, A. Fallarero, P. Shinde, CP Anju, I. Busygin, R. Leino, C.G. Mohan, P. Vuorela, Chemical modifications of cinchona alkaloids lead to enhanced inhibition of human butyrylcholinesterase, Nat. Prod. Commun. 9(4) (2014) 455 – 458.

[9] S.A. Nawaz, M. Ayaz, W. Brandt, L.A. Wessjohann, B. Westermann, Cation–π and π–π stacking interactions allow selective inhibition of butyrylcholinesterase by modified quinine and cinchonidine alkaloids, Biochem. Bioph. Res. Co. 404 (2011) 935–940. https://doi.org/10.1016/j.bbrc.2010.12.084.

[10] L.Y. Lim, M.L. Go, The anticholinesterase activity of mefloquine, Clin Exp Pharmacol Physiol. 12 (1985) 527-531.

[11] S.D. Katewa, S.S. Katyare, Antimalarials inhibit human erythrocyte membrane acetylcholinesterase, Drug Chem. Toxicol. 28 (2005) 467–482. https://doi.org/10.1080/01480540500262912.

[12] L.J. Dawson, V.L. Caulfield, J.B. Stanbury, A.E. Field, S.E. Christmas, P.M. Smith, Hydroxychloroquine therapy in patients with primary Sjögren's syndrome may improve salivary gland hypofunction by inhibition of glandular cholinesterase, Rheumatology 44 (2005) 449–455. https://doi.org/10.1093/rheumatology/keh506.

[13] Y. Chen, Y. Bian, Y. Sun, C. Kang, S. Yu, T. Fu, W. Li, Y. Pei, H. Sun, 2016. Identification of 4-aminoquinoline core for the design of new cholinesterase inhibitors, PeeRJ 4:e2140. https://doi.org/10.7717/peerj.2140.

[14] F. Nachon, P. Masson, Y. Nicolet, O. Lockridge, J. C. Fontecilla-Camps, Comparison of structures of butyrylcholinesterase and acetylcholinesterase, in: E. Giacobini (Ed.), Butyrylcholinesterase, its function and inhibitors, Martin Dunitz Ltd., London, 2003, pp. 39-45.

[15] J.L. Sussman, M. Harel, F. Frolow, C. Oefner, A. Goldman, L. Toker, I. Silman, Atomic structure of acetylcholinesterase from Torpedo californica. A prototypic acetylcholine-binding protein. Science 253 (1991) 872-897. https://doi.org/10.1126/science.1678899.

[16] Y. Nicolet, O. Lockridge, P. Masson, J.C. Fontecilla-Camps, F. Nachon, Crystal structure of human butyrylcholinesterase and of its complexes with substrate and products, J. Biol. Chem. 278 (2003) 41141-41147. https://doi.org/10.1074/jbc.M210241200.

[17] P. Taylor, Z. Radić, The cholinesterases: from genes to proteins, Annu. Rev. Pharmacol. Toxicol. 34 (1994) 281−320. https://doi.org/10.1146/annurev.pa.34.040194.001433.

[18] A. Ordentlich, D. Barak, C. Kronman, Y. Flashner, M. Leitner, Y. Segall, N. Ariel, S. Cohen, B. Velan, A. Shafferman, Dissection of the human acetylcholinesterase active centre determinants of substrate specificity. Identification of residues constituting the anionic site, the hydrophobic site, and the acyl pocket, J. Biol. Chem. 268 (1993) 17083−17095.

[19] Z. Radić, N.A. Pickering, D.C. Vellom, S. Camp, P. Taylor, Three distinct domains in the cholinesterase molecule confer selectivity for acetylcholinesterase and butyrylcholinesterase inhibitors. Biochemistry 32 (1993) 12074-12084. https://doi.org/10.1021/bi00096a018.

[20] Z. Kovarik, Z. Radić, H.A. Berman, V. Simeon-Rudolf, E. Reiner, P. Taylor, Acetylcholinesterase active centre and gorge conformations analysed by combinatorial mutations and enantiomeric phosphonates. Biochem J. 373 (2003) 33-40. https://doi.org/10.1042/BJ20021862.

[21] A. Bosak, I. Gazić, V. Vinković, Z. Kovarik, Amino acids involved in stereoselective inhibition of cholinesterases with bambuterol, Arch. Biochem. Biophys. 471 (2008) 72-76. https://doi.org/10.1016/j.abb.2007.12.007.

[22] A. Bosak, I. Gazić Smilović, A. Štimac, V. Vinković, G. Šinko, Z. Kovarik, Peripheral anionic site and acyl pocket define selective inhibition of butyrylcholinesterase by two biscarbamates, Arch. Biochem. Biophys. 529 (2013) 140-145. https://doi.org/10.1016/j.abb.2012.11.012.

[23] A. Bosak, I. Gazić-Smilović, G. Šinko, V. Vinković, Z. Kovarik, Metaproterenol, isoproterenol, and their bisdimethylcarbamate derivatives as human cholinesterase inhibitors, J. Med. Chem. 55 (2012) 6716-6723. https://doi.org/10.1021/jm300289k.

[24] A. Bosak, I. Primožič, M. Oršulić, S. Tomić, V. Simeon-Rudolf, Enantiomers of quinuclidin-3-ol derivatives: Resolution and interactions with human cholinesterases, Croat. Chem. Acta 78 (2005) 121-128.

[25] Z. Kovarik, A. Bosak, G. Šinko, T. Latas. Exploring active sites of cholinesterases by inhibition with bambuterol and haloxon. Croat Chem Acta. 76 (2003) 63-67.

[26] I. Aleksić, S. Šegan, F. Andrić, M. Zlatović, I. Morić, D. M. Opsenica, L. Šenerović, Long-chained 4-aminoquinolines as quorum sensing inhibitors in *Serratia marcescens* and *Pseudomonas aeruginosa*, ACS Chem. Biol., 12 (2017) 1425-1434. https://doi.org/10.1021/acschembio.6b01149.

[27] B.A. Šolaja, D. Opsenica, K.S. Smith, W.K. Milhous, N. Terzić, I. Opsenica, J.C. Burnett, J. Nuss, R. Gussio, S. Bavari, Novel 4-aminoquinolines active against chloroquine-resistant and sensitive *P. falciparum* strains that also inhibit botulinum serotype A, J. Med. Chem. 51 (2008) 4388–4391. https://doi.org/10.1021/jm800737y.

[28] G.L. Ellman, K.D. Courtney, V. Andres, R.M.A. Featherstone, A new and rapid colorimetric determination of acetylcholinesterase activity, Biochem. Pharmacol. 7 (1961) 88–95. http://dx.doi.org/10.1016/0006-2952(61)90145-9.

[29] P. Eyer, F. Worek, D. Kiderlen, G. Sinko, A. Stuglin, V. Simeon-Rudolf, E. Reiner, Molar absorption coefficients for the reduced Ellman reagent: reassessment, Anal Biochem. 312 (2003) 224-227. http://dx.doi.org/10.1016/S0003-2697(02)00506-7.

[30] V. Simeon-Rudolf, G. Šinko, A. Štuglin, E. Reiner, Inhibition of human blood acetylcholinesterase and butyrylcholinesterase by ethopropazine, Croat. Chem. Acta 74(1) (2001) 173–182.

[31] T. Matsui, T. Baba, K. Kamiya, Y. Shigeta, An accurate density functional theory based estimation of pKa values of polar residues combined with experimental data: from amino acids to minimal proteins. Phys. Chem. Chem. Phys. 14(12) 2012, 4181–4187. https://doi.org/10.1039/c2cp23069k.

[32] T. Matsui, Y. Shigeta, K. Morihashi, Assessment of methodology and chemical group dependences in the calculation of the pKa for several chemical groups. J. Chem. Theory Comput. 13(10) (2017) 4791–4803. https://doi.org/10.1021/acs.jctc.7b00587.

[33] A. Pérez-González, R. Castañeda-Arriaga, B. Verastegui, M Carreón-González, J.R. Alvarez-Idaboy, A. Galano, 2018. Estimation of empirically fitted parameters for calculating

pKa values of thiols in a fast and reliable way. Theor. Chem. Acc. 137:5 https://doi.org/10.1007/s00214-017-2179-7.

[34] A. Galano, A. Pérez-González, R. Castañeda-Arriaga, L. Muñoz-Rugeles, G. Mendoza-Sarmiento, A. Romero-Silva, A. Ibarra-Escutia, A.M. Rebollar-Zepeda, J.R. León-Carmona, M.A. Hernández-Olivares, J.R. Alvarez-Idaboy, Empirically fitted parameters for calculating p*K*a values with small deviations from experiments using a simple computational strategy. J. Chem. Inf. Model. 56(9) (2016) 1714–1724. https://doi.org/10.1021/acs.jcim.6b00310.

[35] S. Zhang, A reliable and efficient first principles-based method for predicting p*K*a values. 4. Organic bases. J. Comput. Chem. 33(31) (2012) 2469–2482. https://doi.org/10.1002/jcc.23068.

[36] A.V. Marenich, C.J. Cramer, D:G: Truhlar, Universal solvation model based on solute electron density and on a continuum model of the solvent defined by the bulk dielectric constant and atomic surface tensions. J. Phys. Chem. B 113(18) (2009) 6378–6396. https://doi.org/10.1021/jp810292n.

[37] M. J. Frisch, G. W. Trucks, H. B. Schlegel, G. E. Scuseria, M. A. Robb, J. R. Cheeseman, G. Scalmani, V. Barone, B. Mennucci, G. A. Petersson, H. Nakatsuji, M. Caricato, X. Li, H. P. Hratchian, A. F. Izmaylov, J. Bloino, G. Zheng, J. L. Sonnenberg, M. Hada, M. Ehara, K. Toyota, R. Fukuda, J. Hasegawa, M. Ishida, T. Nakajima, Y. Honda, O. Kitao, H. Nakai, T. Vreven, J. A. Montgomery, Jr., J. E. Peralta, F. Ogliaro, M. Bearpark, J. J. Heyd, E. Brothers, K. N. Kudin, V. N. Staroverov, R. Kobayashi, J. Normand, K. Raghavachari, A. Rendell, J. C. Burant, S. S. Iyengar, J. Tomasi, M. Cossi, N. Rega, J. M. Millam, M. Klene, J. E. Knox, J. B. Cross, V. Bakken, C. Adamo, J. Jaramillo, R. Gomperts, R. E. Stratmann, O. Yazyev, A. J. Austin, R. Cammi, C. Pomelli, J. W. Ochterski, R. L. Martin, K. Morokuma, V. G. Zakrzewski, G. A. Voth, P. Salvador, J. J. Dannenberg, S. Dapprich, A. D. Daniels, Ö. Farkas, J. B. Foresman, J. V. Ortiz, J. Cioslowski, D. J. Fox, Gaussian 09, Revision D.01. Gaussian, Inc., Wallingford CT. 2009.

[38] S. Grimme, Supramolecular binding thermodynamics by dispersion-corrected density functional theory. Chem. Eur. J. 18 (32) (2012) 9955–9964. https://doi.org/10.1002/chem.201200497.

[39] Funes-Ardoiz, R.S. Paton, GoodVibes: version 2.0.1. 2018.

[40] N.M. O'Boyle, M. Banck, C.A. James, C. Morley, T. Vandermeersch, G.R. Hutchison. 2011, Open Babel: An open chemical toolbox. J. Cheminform. 3:33 https://doi.org/10.1186/1758-2946-3-33.

[41] Y.H. Jang, W.A. Goddard III, K.T. Noyes, L.C. Sowers, S. Hwang, D.S. Chung, p$K_a$ values of guanine in water: density functional theory calculations combined with poisson−boltzmann continuum−solvation model, J. Phys. Chem. B 107(1) (2003) 344–357. https://doi.org/10.1021/JP020774X.

[42] V.S. Bryantsev, S. Mamadou A. Diallo, W:A: Goddard III, p*K*a calculations of aliphatic amines, diamines, and aminoamides via density functional theory with a poisson−boltzmann continuum, Solvent Model. J. Phys. Chem. A 111 (2007) 4422–4430. http://doi.org/10.1021/JP071040T.

[43] M.N. Ngamelue, K. Homma, O. Lockridge, O.A. Asojo. Crystallization and X-ray structure of full-length recombinant human butyrylcholinesterase, Acta Crystallogr F Struct Biol. Cryst. Commun. 63 (2007) 723–727. https://doi.org/10.1107/S1744309107037335.

[44] The protein data bank. http://www.rcsb.org/pdb/explore.do?structureId=4pqe

[45] N. Maraković, A. Knežević, V. Vinković, Z. Kovarik, G. Šinko. Design and synthesis of N-substituted-2-hydroxyiminoacetamides and interactions with cholinesterases. Chem-Biol Interact. 259 (2016) 122–132. https://doi.org/10.1016/j.cbi.2016.05.035.

[46] Chemicalize, calculation module (2/2018), https://chemicalize.com/ developed by ChemAxon (http://www.chemaxon.com)

[47] H. Pajouhesh, G.R. Lenz. Medicinal chemical properties of successful central nervous system drugs, NeuroRx 2 (2005) 541-553. https://doi.org/10.1602/neurorx.2.4.541.

[48] D.D: Perrin, Dissociation constants of organic bases in aqueous solution, Butterworths, London, 1965.

[49] D.C. Warhurst, J.C.P. Steele, I.S. Adagu, J.C. Craig, C. Cullander, Hydroxychloroquine is much less active than chloroquine against chloroquine-resistant *Plasmodium Falciparum*, in Agreement with its physicochemical properties. J. Antimicrob. Chemother. 52(2) (2003) 188–193. https://doi.org/10.1093/jac/dkg319.

[50] H. Dvir, D.M. Wong, M. Harel, X. Barril, M. Orozco, F.J. Luque, D. Muñoz-Torrero, P. Camps, T.L. Rosenberry, I. Silman, J.L. Sussman, 3D structure of Torpedo californica acetylcholinesterase complexed with huprine X at 2.1 A resolution: kinetic and molecular dynamic correlates, Biochemistry. 41(9) (2002) 2970-81. https://doi.org/10.1021/bi011652i.

[51] F. Nachon, E. Carletti, C. Ronco, M. Trovaslet, Y. Nicolet, L. Jean, P.Y. Renard, Crystal structures of human cholinesterases in complex with huprine W and tacrine: elements of specificity for anti-Alzheimer's drugs targeting acetyl- and butyryl-cholinesterase, Biochem J. 453(3) (2013) 393-399. https://doi.org/10.1042/BJ20130013.

[52] J.-P. Colletier, D. Fournier, H.M. Greenblatt, J. Stojan, J.L. Sussman, G. Zaccai, I. Silman, M. Weik, Structural insights into substrate traffic and inhibition in acetylcholinesterase, EMBO J. 25(12) (2006) 2746-2756. https://doi.org/10.1038/sj.emboj.7601175.

[53] U. Košak, B. Brus, D. Knez, R. Šink, S. Žakelj, J. Trontelj, A. Pišlar, J. Šlenc, M. Gobec, M. Živin, L. Tratnjek, M. Perše, K. Sałat, A. Podkowa, B. Filipek, F. Nachon, X. Brazzolotto, A. Więckowska, B. Malawska, J. Stojan, I. Mlinarič Raščan, J. Kos, N. Coquelle, J.-P. Colletier, S. Gobec, 2016. Development of an in-vivo active reversible butyrylcholinesterase inhibitor. Sci. Rep.-UK. 6, 39495. https://doi.org/10.1038/srep39495.

[54] Saxena, J.M. Fedorko, C.R. Vinayaka, R. Medhekar, Z. Radić, P. Taylor, O. Lockridge, B.P. Doctor. Aromatic amino-acid residues at the active and peripheral anionic sites control the binding of E2020 (Aricept) to cholinesterases. Eur. J. Biochem. 270 (2003) 4447–4458. https://doi.org/10.1046/j.1432-1033.2003.03837.x.

[55] A. Brus, U. Kosak, S. Turk, A. Pislar, N. Coquelle, J. Kos, J. Stojan, J.P. Colletier, S. Gobec, Discovery, biological evaluation, and crystal structure of a novel nanomolar selective butyrylcholinesterase inhibitor, J. Med. Chem. 57(19) (2014) 8167-8179. https://doi.org/10.1021/jm501195e.

[56] E. Giacobini, Selective inhibitors of butyrylcholinesterase. A valid alternative for therapy of Alzheimer's disease? Drug. Aging 18 (182) (2001) 891-898. https://doi.org/ 10.2165/00002512-200118120-00001.

**Figure Legends**

**Fig. 1.** Chemical structure of the tested compounds.

**Fig. 2.** Orientation of ligands in the active site of AChE. Position of ligand **CQAd** (A) and ligand **TFQ8** (B). Interactions are presented in green (H-bonds), orange (cation-π interaction), and purple (hydrophobic interactions).

**Fig. 3.** Position of ligand **CQEtOH** (A) and ligand **CQ2** (B) in the active site of BChE. Interactions are presented in green (H-bonds), orange (cation-π interaction), and purple (hydrophobic interactions).

**Fig. 4.** Comparison of ligand **CQ8** orientations in the active site of cholinesterases. Position of ligand in AChE (A) and in BChE (B). Interactions are presented in green (H-bonds), orange (cation-π interaction) and purple (hydrophobic interactions).

**Scheme 1.** Synthesis of 4-aminoquinoline derivatives.

**Highlights**

- three derivatives were nanomolar selective AChE inhibitors
- the quinoline group is primarily stabilised by the choline binding site residues
- 4-aminoquinoline derivatives exhibit slight selectivity toward AChE over BChE
- 4-aminoquinoline derivatives have potential to penetrate the blood brain barrier

**Submission no: CHEMBIOINT_2019_371_R2**
**Submission title: Structural aspects of 4-aminoquinolines as reversible inhibitors of human acetylcholinesterase and butyrylcholinesterase**
**Journal: Chemico-Biological Interactions**

**Declaration of interests**

☒ The authors declare that they have no known competing financial interests or personal relationships that could have appeared to influence the work reported in this paper.

☐The authors declare the following financial interests/personal relationships which may be considered as potential competing interests:

Corresponding author:

Anita Bosak

Dr. Anita Bosak
on behalf of all the authors

Zagreb, April 24, 2019